Case Studies in Thermal Engineering 33 (2022) 101925

Contents lists available at ScienceDirect

Case Studies in Thermal Engineering

journal homepage: www.elsevier.com/locate/csite

Experimental study and mathematical model development for the effect of water depth on water production of a modified basin solar still

Mahmoud S. El-Sebaey [a,*], Asko Ellman [b], Ahmed Hegazy [a], Hitesh Panchal [c]

[a] Mechanical Power Engineering Department, Faculty of Engineering, Menoufia University, Shebin El-Kom, Egypt
[b] Faculty of Engineering and Natural Sciences, Tampere University, Finland
[c] Mechanical Engineering Department, Government Engineering College Patan, Gujarat, India

ARTICLE INFO

Keywords:
Single-slope double-basin still
Basin depth
Internal heat transfer coefficient
Freshwater
Efficiency

ABSTRACT

Freshwater is constantly shrinking with the confindness of water resources. Therefore, desalination of seawater is given great attention. Renewable energy sources also become of high importance to reduce carbon emissions. Thus, this study is concerned with the design, fabrication, and testing of a new single-slope double-basin solar still as a renewable energy-driven desalination system. It differs from the conventional solar stills by having two basins. The experiments were conducted to compare the performance of both conventional and modified solar stills. As a design parameter that substantially affects the performance, the still water depth was investigated. A new straightforward, accurate model is developed to predict both systems' performance for the design and optimization within a maximum deviation of ±6.6%. The results indicated that the day's productivity for the new and conventional stills at 2 cm water depth was 2.855 and 1.785 L/m^2 per day, respectively, by an increase of 59.9% with a thermal efficiency improvement of 61.3%. Also, a rise in the equivalent water depth d_e from 2 cm to 3 cm reduces the accumulated productivity by 14.36% and 15.41% for the SSDBSS and SSSS, respectively. Additionally, the daily thermal efficiency of the SSDBSS and SSSS is 25% and 15.5% for water depth d_e of 2 cm, respectively. The maximum values of the total heat transfer coefficient were also evaluated to be 15.4 and 55 W/m^2.°C for the lower and upper basins of the modified system, respectively, and 30.18 W/m^2.°C for the conventional system.

Nomenclature

C, n	Nusselt number expression unknown constants —
d_e	Equivalent water depth in the basins of the SSDBSS cm
d_l	Water depth in the lower basin of the SSDBSS cm
d_s	Water depth in the basin of the SSSS cm
d_u	Water depth in the upper basin of the SSDBSS cm
Gr	Grashof number —
h_{cw}	Coefficient of heat transfer by convection from water surface to glass cover W/m^2.K

* Corresponding author.
E-mail address: eng_mahmoudelsebaey@yahoo.com (M.S. El-Sebaey).

https://doi.org/10.1016/j.csite.2022.101925
Received 16 January 2022; Received in revised form 3 March 2022; Accepted 7 March 2022
Available online 14 March 2022

h_{ew}	Coefficient of heat transfer by radiation from water surface to the glass cover W/m^2.K
K_v	Thermal conductivity of the humid air W/m K
L	Latent heat of water vaporization J/kg
L_v	Mean distance between the glass cover and water surface M
Nu	Nusselt number —
P_g	Vapor pressure at the glass surface temperature N/m^2
P_w	Vapor pressure at the water surface temperature N/m^2
Pr	Prandtl number —
$\dot{q}_{ew}$	Rate of energy lost from the water surface by evaporation W/m^2
R	Parameter —
Ra	Rayleigh number —
T_g	The temperature of the glass cover °C
T_v	The temperature of the water vapor °C
T_w	Temperature of water °C
L_v	Mean distance between the glass cover and water surface M

Abbreviations

SSDBSS	Single-Slope Double-Basin Solar Still
SSSS	Single-Slope Solar Still
MSF	Multi-Stage Flash
MED	Multiple Effect Distillation
TVC	Thermal Vapor Compression
MD	Membrane Distillation
RO	Reverse Osmosis
PVC	Chloride Vinyl Poly
UNICEF	United Nations Children's Emergency Fund

1. Introduction

A solar still is an important device for using solar energy to turn saltwater water into drinkable water. [1]. It is inexpensive, cost-effective, and requires less skilled labour to manufacture than other desalination technologies [2]. Because the distillate output received by the solar still remains lower, therefore it is not an essential device for supplying potable water to industry and households in large quantities [3].

There have been several attempts by researchers worldwide to improve the distillate yield of the solar still, using a variety of methods or ideas [4]. Higher water temperature and lower inner glass cover temperature are considered driving forces to enhance the distillate output of solar still [5]. Researchers have experimented with various methods to raise the temperature of the water in the solar still. The solar collector is an important device that is used with the solar still to feed hot water to the solar still's a basin. O.O. Badran and H.A.Al-Tahaineh [6] conducted a series of tests on a solar still equipped with a flat plate collector at various depths of water. According to their findings, a flat plate collector coupled with a solar still increased distillate output by 36%. Mevada et al. [7] tested the performance of solar still with and without using the evacuated tubes and condenser in climate conditions of Gandhinagar, Gujarat, India. They also conducted exergo economic and exergo environmental analysis of both solar stills systems. Artificial intelligence model and moth-flame optimizer were used to forecast the productivity of a solar distiller, which was integrated with evacuated tubes and an external condenser by ammar el sheikh et al. [8]. To determine the influence of flat plate collector coupling on distillate yield, Badran et al. [9] conducted 24-h experiments with a solar still that used tap water and saltwater, as well as a coupling of a flat plate collector. They discovered that coupling a flat plate collector to tap water and saline water resulted in 52% and 231% distillate yields, respectively. A flat plate collector integrated with a solar still was tested in the climate of Madurai, India, by Rajaseenivsan et al. [10]. A 30% improvement in distillate yield was observed when an integrated flat plate collector was used compared with conventional solar still, as reported by the researchers. An experimental examination of the performance of a solar water distiller that uses a circular parabolic absorber has conducted by Samir M. Elshamy et al. [11]. They concluded that the solar distiller with a circular parabolic absorber had an excellent design and excellent performance and productivity. Morad et al. [12] used a solar still with a flat plate collector and tested it in Egyptian climate conditions, both with and without cooling effect. They discovered that using a flat plate collector coupled with glass cover cooling is the most effective technique to improve solar still production. Singh et al. [13] carried out a performance evaluation of evacuated tubes integrated with solar stills in natural circulation mode [13]. They carried out the experiments with a constant water depth of 0.03 m. The results of the experiments were utilized to calculate energy and exergy efficiencies. Panchal et al. [14] had reviewed several papers on using Computational fluid dynamics in solar still. They concluded that computational fluid dynamics is an excellent tool to predict the performance of the solar still. Shiv Kumar et al. [15] had employed evacuated tubes coupled with a solar still operating in the forced circulation mode. In addition, they estimated the system's thermal performance, validated their predicted results against the experimental data, and received good agreement. The distillate output of a solar still coupled with evacuated tubes in forced circulation mode was more significant than the natural circulation mode. Shafil et al.

[16] used a unique design of evacuated tubes in conjunction with solar still and thermoelectric modules. Thermoelectric generators produce enough electricity to power the propeller fan for forced circulation to enhance heat transfer. As a result of their experiments achieved the maximum distillate output of 1.11 kg/m^2/hr as a result of their investigations. Kamran Mohammadi et al. [17] had used a novel design of the multi-scale heat exchanger with parabolic trough coupled solar still and tested in climate conditions of Iran. They found that the novel design of heat exchangers found 39.4% highest overall efficiency from experimental work. A heat and mass transfer of integrated solar still with an underground heat exchanger simplified model was presented by Salman H. Hammadi [18]. For both the solar still and the underground heat exchanger, the model contains a theoretical study in the transient mode, which is applicable throughout the year in a warm climatic zone. Three active single slope solar stills have been subjected to a computational study on the basis of energy and exergy have compared by Joshi and Tiwari [19]. In terms of energy efficiency, the strategy preferred by them has plenty of space to increase exergy efficiency further. Mahmoud S El-Sebaey et al. [20] had conducted the comparison between the CFD simulation and Experimental analysis of the double slope solar still. They found good agreement between the CFD simulation and Experimental results of double slope solar still. Similarly Mahmoud S. El-Sebaey et al. [21] carried out similar study on the single slope solar still and received good agreement too.

2. Experimental setup

Fig. 1 presents a schematic diagram of the experimental setup for both solar stills studied in the current work, conventional single-slope solar still (SSSS) and single-slope double-basin solar still (SSDBSS). The SSSS has only one internal body part, while the SSDBSS comprises two internal body parts, i.e., the lower and upper ones. The lower body part of the SSDBSS has the same shape as the SSSS body. Both internal bodies are constructed of galvanized iron sheets with a thickness of 0.8 mm. The internal base of each body has the dimensions of 1000 × 1000 mm. They have rectangular-shaped front and rear sides with heights of 100 and 525 mm, respectively. The sidewalls are made as trapezoidal shapes with smaller and larger heights of 100 and 525 mm, respectively; these heights allow the upper edges of the sidewalls to have a slope of 23°. The still walls are welded to each other and the still base at the corresponding edges constituting the cavity of the SSSS and the lower internal body part of the SSDBSS. The base and walls of each still internal body part are enclosed by a wooden box having the exact shape of both still parts with inner dimensions a little bit greater than the outer dimensions of the still bodies to allow inserting the still internal parts inside the wooden boxes. The wooden boxes have a thickness of 50 mm and serve as thermal insulators to diminish heat loss from the still sides and base. Two PVC tubes of diameter 1" (25.4 mm) are inserted through two holes in the sidewalls of the wooden enclosures and internal still bodies. Both tubes are fixed to the sidewalls of the inner body sides using adhesive silicone rubber glue; one tube lies at a distance of 60 mm above the base, and the other lies directly on the base and is used for draining the brine.

The upper internal body part of the SSDBSS is made in the shape of a parallelepiped from 3 mm thickness acrylic sheet where its base has the dimensions of 1100 × 1195 mm. The walls of the upper internal body part of the SSDBSS are made with a height of 100 mm. The length of the frontal and rear walls is 1000 mm, and the side walls have a length of 1095 mm. The front and rear walls are fixed vertically to the base using adhesive silicone rubber glue, 50 mm from the lower and upper edges, respectively. The side walls are made as parallelograms, and they stick to the base, front and rear walls using adhesive silicone rubber glue. It is to be noticed that the side walls are 50 mm from the base side edges. Ten equally spaced vertical Acrylic strips of 50 mm height and 3 mm thickness were fitted to the cavity of the upper part parallel to the frontal and rear walls. They are fixed to the base of the cavity and side walls using adhesive silicone rubber glue and serve to hold saltwater. The upper still internal body part of the SSDBSS was left without coating to lose its translucence and allow the incident solar radiation to penetrate to the lower part of the still. A wooden box was installed around

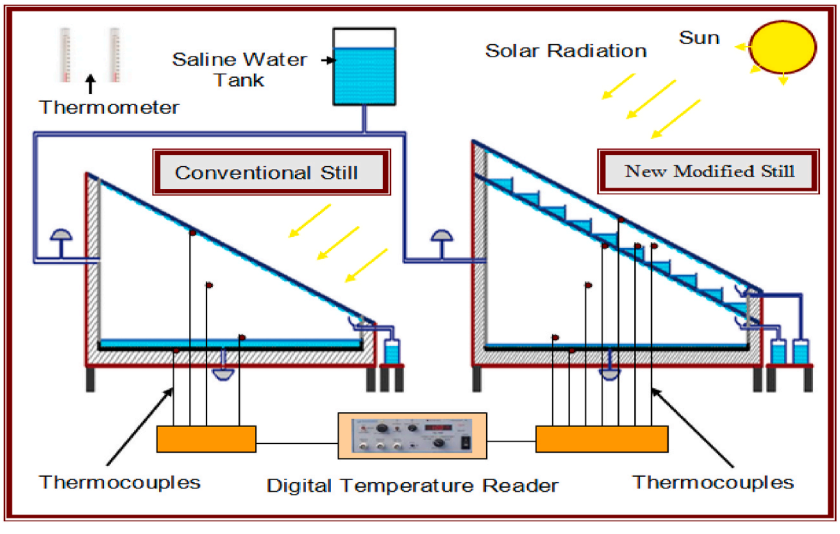

Fig. 1. A schematic diagram of the experimental setup of the single and double basin, single slope solar stills.

the front, rear, and sidewalls of the upper part for easy assembly and installation of the SSDBSS.

Ten tubes with 10 mm diameter were inserted through holes in one side of both the wooden box and upper still body of the SSDBSS. They are fixed to the inner surface, using adhesive silicone rubber glue at a distance of 40 mm from the lower edge of each compartment. These tubes are fitted with valves for allowing saltwater to flow into the compartments of the upper still internal body part and prevent the air from the stream outside this still part. Similar ten tubes are fitted to the other sidewall but at the lowest position of each compartment for draining the brine. The top still body part, along with the wooden box, was set on the sidewalls of the lower part. To prevent any air penetration inside the lower still body part of the SSDBSS to the surroundings, the borders of the separating surface between the upper and lower parts of the still are sealed using adhesive silicone rubber glue. The base of the upper part acts as a condensing surface for the lower part. All surfaces of the wooden enclosures were painted with soft polymer polyester putty 351 to seal them against air and water.

The top of the condensing covers of both the SSSS and the upper internal body part of the SSDBSS was made of transparent window glass with a thickness of 3 mm. They are fixed on the still upper edges of the wooden enclosure and still internal bodies using adhesive silicone rubber glue.

For collecting the distillate from each of the SSSS and the lower still part of the SSDBSS, a 1" (25.4 mm) diameter half PVC tube, with a length equal to the internal length of the frontal still side, is fixed 5 mm below the upper edge of the frontal still side using adhesive silicone rubber glue. This half tube extends from one lateral side of the still to the other and tilted 10° to the horizontal. A 1" (25.4 mm) diameter complete tube is inserted through a hole in the wooden enclosure along with the still body. It is fixed to the internal surface of the still frontal side, at the lower terminal of the collecting tube, using adhesive silicone rubber glue. This tube is connected to a vertical tube of 1″ diameter through an elbow and conveys the distillate to the collecting tank. The same system collects the distillate from the upper internal still body.

Fig. 2 exhibits a photograph of the experimental setup. The solar radiation passes through the top glass covers to the stills, where the black bases absorb most of this radiation. Water starts heating up, and the air moisture inside the stills increases due to water evaporation. The bases radiate infra-red radiation reflected in the stills by the transparent covers to be trapped inside the still. Heated water vapor condenses on the internal surfaces of the cooler condensing covers. Condensed water goes down the inclined condensing covers to inside the collection trough, fixed at the lower edge of the covers to collect the freshwater. The distillate is collected and continuously drained through a plastic tube and stored in external measuring jars. Holes in the SSSS and lower part of SSDBSS back walls are provided for the water inlet to keep the heights of the water in the basins invariable. Other holes in the side walls allow inserting the thermocouples for measuring the temperatures of the inner condensing covers, water vapor, water, and the base of the basins. Also, two holes in the base of the basins are fitted for brine exit and a transparent U tube manometer to ensure that the basin's saltwater height remains constant.

The orientation of the solar stills was to the south to receive the largest possible solar radiation during the experiments. The stills basins were cleaned regularly to evade the deposition of salts.

3. Experimental procedure

The current experimental investigation has been performed using two manufactured solar still models in the laboratory of solar energy of Menoufia University (latitude of 30.5° N and longitude 31.01° E), Egypt. Experiments for predicting the performances of the stills were carried out during June and July 2018. Each test started at the local time of 07:00 and continued until 20:00. The comparative performances of the two constructed solar stills were analyzed for a constant amount of saline water at the start of the test at 20, 30, 40, and 50 L for escaping the effect of water depth on freshwater productivity. The experimental tests were done over ten days for every water depth. In the course of testing the stills, on switching over from one water volume to another, the solar stills were left idle, at least for one day, to attain steady-state conditions before starting the experiment for the following water depth.

Fig. 2. A photograph of the experimental setup.

4. Experimental uncertainty

Some uncertainties may stem from instrument selection, calibration, environment, and reading. The instruments' measured uncertainty values are considered plus or minus (±) half the smallest scale division. For each solar still, the following parameters were measured each hour: the global solar radiation, ambient air temperature, and distillate yield, besides the temperatures of inner glass cover surface, vapor, water, and the basin. On measuring these parameters the uncertainties, which may occur, are presented in Table 1.

5. Evaluation of distillate output

The following thermodynamic analysis is carried out for SSSS. This analysis is valid for the modified solar still SSDBSS, which will be clarified later in this section.

The hourly distillate output per meter square of the solar still can be assessed by:

$$\dot{M}_w = \frac{\dot{q}_{ew} \times 3600}{L} \tag{1}$$

where $\dot{q}_{ew}$ is the rate of water evaporation heat and L is the latent heat of water vaporization.

The hourly productivity rate can also be expressed as [20]:

$$\dot{M}_w = \frac{h_{ew}\left(T_w - T_g\right) \times 3600}{L} \tag{2}$$

where T_w and T_g are the temperatures of water surface and glass cover, respectively, and h_{ew} is the coefficient of heat transfer by evaporation. This coefficient is defined by [22]:

$$h_{ew} = 16.273 \times 10^{-3} h_{cw} \left(\frac{P_w - P_g}{T_w - T_g}\right) \tag{3}$$

The latent heat of water evaporation can be approximated by the following relation [23]:

$$L = 31.615 \times 10^5 \left[1 - \left(7.6166 \times 10^{-4} T_w\right)\right] \tag{4}$$

where, T_w is measured in Kelvin.

Based on Eqs. [1–3], it can be derived that:

$$\dot{q}_{ew} = 16.273 \times 10^{-3} h_{cw}\left(P_w - P_g\right) \tag{5}$$

The heat transfer coefficient by convection (h_{cw}) from the water to glass cover can be identified based on measured values of distillate output ($\dot{M}_w$) as well as temperatures at the water surface (T_w) and glass cover (T_g). This is calculated by finding out constants n and C involved in the equations representing Nusselt, Rayleigh, Grasshof, and Prandtl numbers (*Nu*, Ra, *Gr*, and Pr), [24]:

$$Nu = C[Ra]^n \tag{6}$$

$$Nu = \frac{h_{cw} L_\nu}{k_\nu} = C[Ra]^n = C[Gr.\mathrm{Pr}]^n \tag{7}$$

$$h_{cw} = \frac{k_\nu}{L_\nu} C[Gr.\mathrm{Pr}]^n \tag{8}$$

Substituting h_{cw} from Eq [8]. into Eq. [5], the rate of evaporative heat transfer from the water to the transparent cover is calculated by:

$$\dot{q}_{ew} = 16.273 \times 10^{-3} \frac{k_\nu}{L_\nu} C[Gr.\mathrm{Pr}]^n \left(P_w - P_g\right) \tag{9}$$

$$Gr = \frac{g\beta L_\nu^3 \rho^2 \Delta T'}{\mu^2} \tag{10}$$

Table 1
Uncertainties of the measured parameters.

Device	Parameter	Range	Uncertainty
Eppley Pyranometer	Solar Radiation	0: 2000 W/m^2	±10 W/m^2
Digital Reader Chromel-Alumel Thermocouple (Type-K)	Temperature	0 : 100 °C	±0.05 °C
Mercury Thermometer	Temperature	0: 100 °C	±0.5 °C
Graduated Jar	Water Volume Productivity	0: 50 ml	±0.5 ml

The effective temperature difference $\Delta T'$ is calculated by:

$$\Delta T' = T_w - T_g + \frac{(P_w - P_g)(T_w + 273)}{268.9 \times 10^3 - P_w} \tag{11}$$

$$Pr = \frac{\mu C_P}{K_v} \tag{12}$$

It can be concluded from Eqs [1,9]. that the hourly distillate output ($\dot{M}_w$) can be expressed as:

$$\dot{M}_w = 16.273 \times 10^{-3} \frac{k_v}{L_v} C[Gr.\mathrm{Pr}]^n (P_w - P_g) \times \frac{3600}{L} \tag{13}$$

Introducing a new parameter (R) which is constant in the steady-state condition and given by:

$$R = 16.273 \times 10^{-3} \frac{k_v}{L_v} (P_w - P_g) \frac{3600}{L} \tag{14}$$

It follows that $\dot{M}_w$ is expressed as a function of R, *Gr* and Pr numbers by:

$$\dot{M}_w = RC[Gr.\mathrm{Pr}]^n \tag{15}$$

$$\frac{\dot{M}_w}{R} = C[Gr.\mathrm{Pr}]^n \tag{16}$$

The logarithm of the two sides of Eq [16]. leads to a linear equation [25]:

$$y = mx + C_o \tag{17}$$

The unknown parameters C and n in Eq [16]. are determined by regression analysis using experimental data of distillate output ($\dot{M}_w$) as well as temperatures of water surface (T_w) and glass cover (T_g), where

$$y = \ln\left(\frac{\dot{M}_w}{R}\right), \cdot C_O = \ln C, \cdot x = \ln(Gr\mathrm{Pr}) \text{and} \cdot m = n$$

With the aid of linear regression analysis, the coefficients m and C_O of Eq [17]. can be calculated as:

$$m = \frac{N(\sum xy) - (\sum x)(\sum y)}{N(\sum x^2) - (\sum x)^2} \tag{18}$$

$$C_O = \frac{(\sum y)(\sum x^2) - (\sum x)(\sum xy)}{N(\sum x^2) - (\sum x)^2} \tag{19}$$

where N is the number of experiments for the steady condition.

The values of C and n are then given as:

$$C = \exp(C_O) \cdot \text{and} \cdot n = m \tag{20}$$

All the analysis is given by Eqs [1–20]. can be applied to each body part of the SSDBSS. Considering the lower part, the only change is that the temperature Tub replaces the temperature Tg of the glass cover on the upper internal part base. As for the upper inner body part of the SSDBSS, the water surface is considered one flat surface with the sum of all surface areas in all compartments of the upper basin with an average temperature T_{uw}. This area exchanges heat with the glass cover via radiation and convection.

6. Internal heat transfer

The heat exchange from the evaporating water surface to the condensing glass cover represents the internal heat transfer inside the solar still. It is governed by heat transfer coefficients of radiation, convection, and evaporation. Hence, the sum of all these coefficients leads to the total heat transfer coefficient (u_i) from the evaporative surface to condensing surface:

$$u_i = h_{cw} + h_{rw} + h_{ew} \tag{21}$$

where h_{rw} is the heat transfer coefficient by radiation.

The heat transfer coefficient by radiation is given by the following relation [22]:

$$h_{rw} = \frac{\varepsilon_{eff}\sigma\left[(T_w + 273)^4 - (T_g + 273)^4\right]}{(T_w - T_g)} \tag{22}$$

where ε_{eff} is the effective emittance between the water surface and glass cover and σ is the Stephan-Boltzman constant, which is equal to 5.67×10^{-8} W/m^2. K^4.

The ε_{eff} among the water and the glass surfaces can be calculated by:

$$\varepsilon_{eff} = \left[\frac{1}{\varepsilon_w} + \frac{1}{\varepsilon_g} - 1\right]^{-1} \tag{23}$$

where ε_w and ε_g are the emittance of water surface and glass cover, respectively, and they have the values of $\varepsilon_w = 0.96$ and $\varepsilon_g = 0.88$, [24].

7. Thermal efficiency

The daily thermal distillation efficiency, (η_d), was determined by summing the hourly outcome ($\dot{M}_w$), multiplied by the latent water heat (L), and divided by the average solar radiation over the day I(t) over the whole base area (A) of the still [26]:

$$\eta_d = \frac{\sum \dot{M}_w \times L}{\sum I(t) \times A} \times 100 \tag{24}$$

8. Results and discussion

The solar radiation and ambient temperature variations were measured during 14.6.2018, as shown in Fig. 3. It is observed from the figure that the solar intensity increased gradually with the local daytime from sunrise, reaching an extreme value of 946 W/m^2 at 12:00, and then it decreased till sunset. The ambient air temperature attained its maximum value around 14:00 that may be referred to as the thermal inertia of the ambient air mass.

To be able to compare the performance of the two studied still configurations, the amount of the saltwater to be desalinated in each still at the start of operation was kept equal. For the SSSS, the whole saltwater amount was held in the still basin, while in the case of SSDBSS, half this amount was contained in the lower still basin, and the other half amount was poured equally into the compartments of the upper basin. Hence, the depth d_s of the saltwater in the SSSS was double the depth d_l of the saltwater in the lower basin of the SSDBSS. For the sake of comparison, an equivalent depth d_e is introduced, which is the depth of saltwater if the whole amount of saltwater is contained inside the lower basin of SSDBSS. The variation of the measured basin, water, vapor, and glass cover temperatures for the SSSS and SSDBSS with day time for water depth d_s and d_e of 2 cm are shown in Figs. 4 and 5, respectively.

It is seen from Figs. 4 and 5 that the water temperature is higher than that of both the temperatures of vapor and the condensing surface, whereas it is lower than the basin temperature. Also, it can be noticed that the water temperature rises gradually with time and reaches a maximal value in the afternoon period between 13:00 and 14:00. This is because of increasing the absorbed solar intensity that surpasses the losses to the surrounding atmosphere. After 14:00, the solar radiation intensity (Fig. 3) and the water temperature decrease accordingly. This is ascribed to the losses from the still cover to the surroundings, which become higher than the absorbed solar radiation. In the morning, the difference in the temperature of the water surface and the condensing surface is relatively small because of the low solar radiation intensity that affects little yield productivity. Also, it can be noted that the temperature of the water attains higher values faster than the condensing cover; this can be referred to as the more thermal heat capacity of water compared to that of the glass cover. Fig. 4 exposes that the maximum temperature of the water is 77.4 °C in the case of SSSS. Fig. 5 suggests clearly

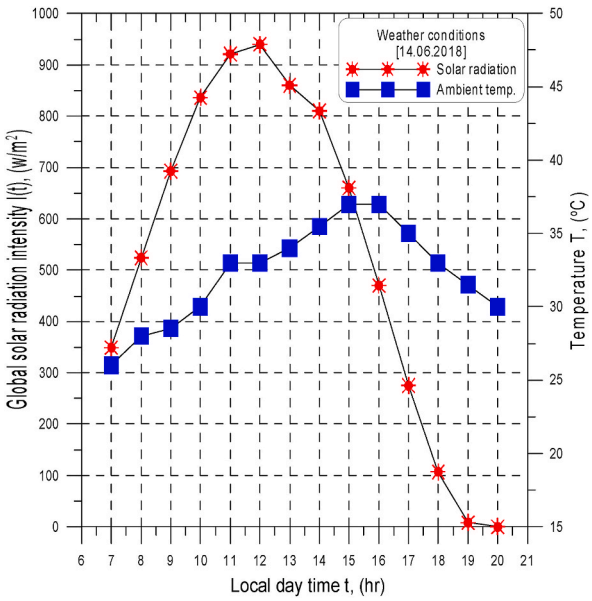

Fig. 3. Variations of solar radiation and dry bulb temperature during 14.06.2018.

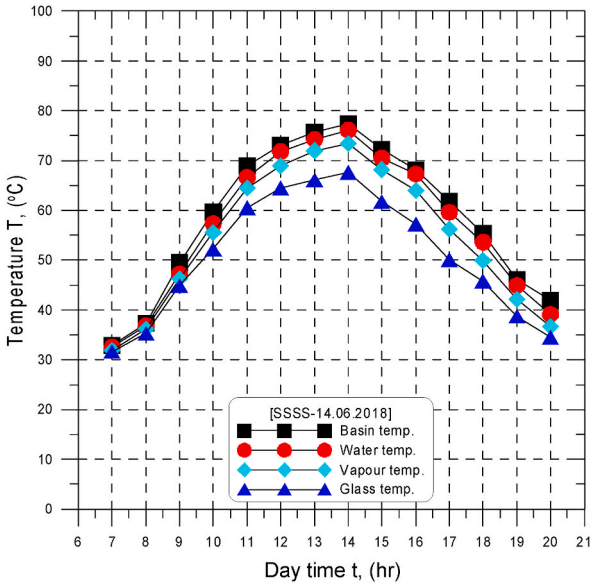

Fig. 4. Hourly variations of the basin, water, vapor, and condensing cover temperatures for SSSS with daytime at water depth d_s of 2 cm.

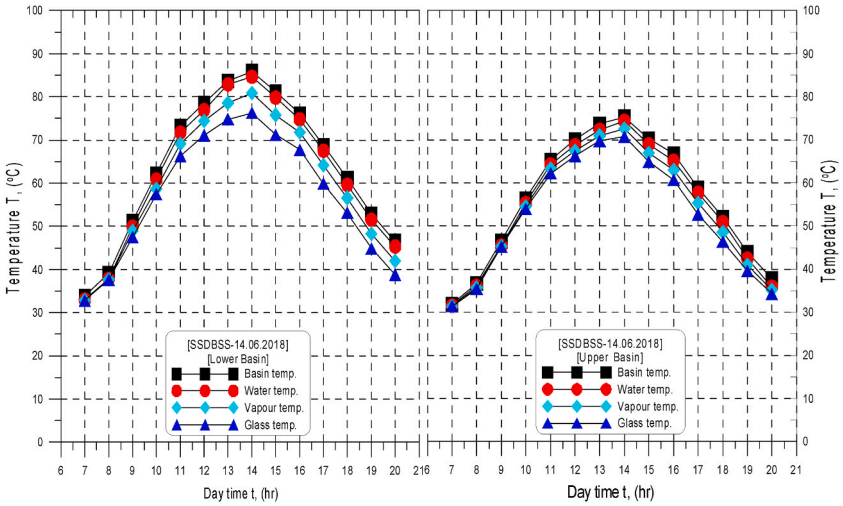

Fig. 5. Hourly variations of the basin, water, vapor, and condensing cover temperatures for SSDBSS with day time at equivalent water depth d_e of 2 cm.

that in the status of the SSDBSS, the maximum water temperature reaches the value of 85.6 °C and 74.4 °C in the lower basin and upper basin, respectively. The purpose of the variation among the values of the temperature of the SSDBSS and the SSSS is to divide the saltwater into two basins, which reduces the water thermal capacity and shrinkage of the air gaps volume of the SSDBSS.

In the distillation process, the values of internal heat transfer coefficients are essential in evaluating system performance. Fig. 6 explains the hourly difference of the coefficients of the internal heat transfer inside the still, namely evaporation (h_{ew}), heat transfer coefficient (these coefficient is calculated using Eq. (3), depending on measured values of hourly productivity, water, and condensing cover temperatures). The coefficients namely evaporation (h_{ew}), convection (h_{cw}), and radiation (h_{rw}) are obtained for water depth d_s/ equivalent water depth d_e of 2 cm for both tested solar still configurations.

It has been demonstrated that the mass transfer rate of evaporation is mightily affected by the heat transfer coefficient of evaporation, and it rises when the heat transfer coefficient of evaporation is raised. This can be attributed to the fact that the solar still output is relative to the evaporation mass transfer rate of water, which depends on the values of the evaporation heat transfer and the variation among temperatures of water and condensing cover surface. This can be seen from the corresponding amounts of heat transfer coefficient by evaporation (h_{ew}) shown in Fig. 6 and the still productivity that will be illustrated in Fig. 7.

Fig. 6 suggests that the highest values of h_{ew} along the day are in the upper basin of the SSDBSS due to the extreme received solar energy, and hence the maximum outcome is obtained. On the other hand, it is noted that the value of h_{ew} is relatively low in the lower

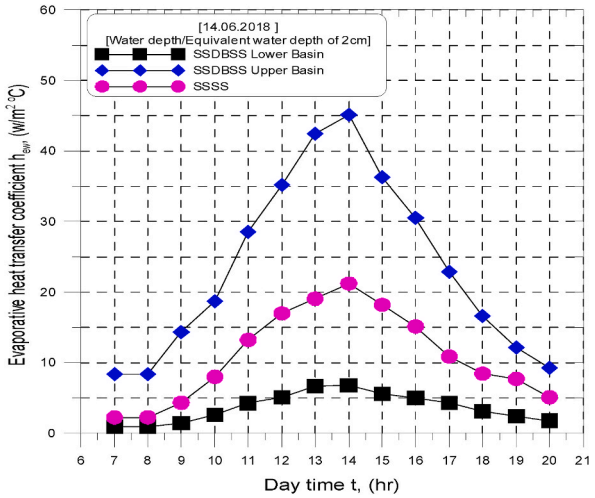

Fig. 6. Hourly variation of heat transfer coefficient by evaporation (h_{ew}) for the SSSS with saltwater depth d_s of 2 cm and the SSDBSS with equivalent depth d_e of 2 cm.

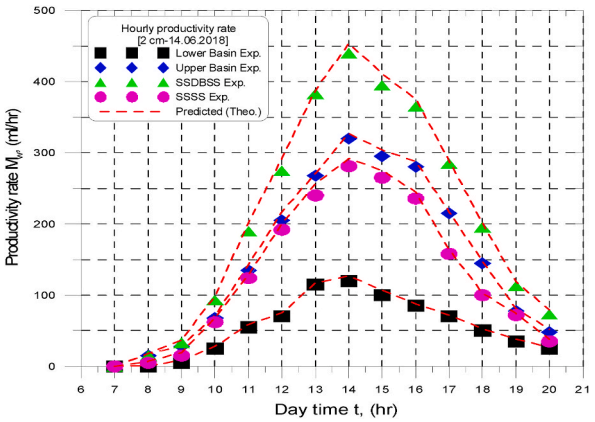

Fig. 7. Hourly variations of experimental and theoretical accumulated freshwater for the SSSS with saltwater depth d_s of 2 cm and the SSDBSS with equivalent depth d_e of 2 cm.

basin of the SSDBSS (Fig. 6) that leading to lower hourly productivity, as will be displayed in Fig. 10. However, the lower basin has the maximum water temperature and the temperature variation among the water and condensing surface, as shown in Figs. 5 and 6, and as will be exhibited in Fig. 10. This is because the still output results from the heat transfer coefficient by evaporation and the temperature variation, and if any of these two values are low, the output will be low too (Eq. (2)).

The heat transfer coefficient by convection has the lowest value along the test period for the two solar stills. Furthermore, the heat transfer coefficient by evaporation throughout the day represents the highest value compared to the heat transfer by radiation and

Table 2
The empirical correlations proposed for depicting heat transfer for the SSSS and SSDBSS with different saltwater depths d_s/d_e.

Type	Water Depth d_s/Equivalent Water Depth d_e	Empirical Correlations	C	n	R^2	Ranges (*Gr*.Pr)
SSSS	2 cm	$Nu = C[GrPr]^n$	0.97199	0.12181	0.98	2.7×10^6–4.0×10^7
	3 cm		0.82407	0.11501	0.99	1.8×10^6–4.3×10^7
	4 cm		0.79917	0.10822	0.98	8.5×10^5–4.3×10^7
	5 cm		0.78682	0.11119	0.97	5.4×10^5–4.1×10^7
SSDBSS Lower Basin	2 cm		0.85303	0.05766	0.97	6.5×10^5–5.9×10^7
	3 cm		0.85889	0.05134	0.98	1.6×10^6–5.9×10^7
	4 cm		0.85566	0.04333	0.97	1.2×10^6–5.9×10^7
	5 cm		0.82515	0.03641	0.98	6.1×10^5–6.2×10^7
SSDBSS Upper Basin	2 cm		1.01078	0.14993	0.98	3.9×10^4–6.5×10^5
	3 cm		1.0180	0.05134	0.99	4.4×10^4–6.6×10^5
	4 cm		1.03521	0.12559	0.98	3.3×10^4–7.0×10^5
	5 cm		0.99528	0.11823	0.99	1.5×10^4–8.2×10^5

convection for the two tested solar still configurations.

The radiative heat transfer depends fundamentally on water temperatures and condensing surface. This mode of heat transfer dominates at the lower basin of the SSDBSS during the whole sunshine period due to the relatively large values of saltwater surface temperature. This is why the amounts of h_{rw} high for the lower basin of the SSDBSS compared with the upper basin and the SSSS. It can also be inferred that the extreme amounts of the total heat transfer coefficient (u_i) -calculated using Eq. 21- were 15.4 and 55 W/m^2.°C for the lower and upper basin of the SSDBSS, respectively and 30.18 W/m^2.°C for the SSSS.

The solar still performance can be estimated accurately when rigorous expressions are utilized for determining the heat transfer coefficients. The proposing empirical correlations for the two tested solar stills with different tested water depths d_s/equivalent water depths d_e are shown in Table 2. The values of the constants C and n and the range of parameter (*Gr*.Pr) are also presented. The worth of the empirical correlations is featured by the potential of determining the heat transfer coefficient h_{cw} (Eq. (8)) with good accuracy. The empirical correlations proposed could be utilized to forecast the freshwater productivities (Eq. (2)) for the two tested solar stills with acceptable accuracy by determining the evaporative heat transfer coefficient h_{ew} (Eq. (3)).

The hourly changes of the experimental and theoretical accumulated freshwater per unit area of the SSSS with saltwater depth d_s of 2 cm and for the SSDBSS with equivalent depth d_e of 2 cm are shown in Fig. 7. The theoretical (predicted) productivity (Eq. (2)) is determined by utilizing the constants C and n of the proposed empirical correlations shown in Table 2 to calculate the coefficient of convection heat transfer h_{cw} (Eq. (8)) and the coefficient of evaporation heat transfer h_{ew} (Eq. (3)) based on the measured temperatures of water, acrylic and glass covers. Fig. 7 displays the same trend as in Figs. 4 and 5; there is a rise in the accumulated freshwater output through the morning of the day until it gets a peak value at 14:00 where the maximum irradiation of the sun occurs, and then a decrease is noticed due to the continuous diminution of solar radiation until it reaches zero at sunset. At a higher basin water temperature, more water evaporates, and the mass of water contained in the air of the still becomes higher. Hence, the maximum output occurs at the maximum measured temperature of saltwater at 14:00. Also, it can be seen from Fig. 7 that there are acceptable agreements among the experimental results and theoretical outcomes for both tested solar stills (SSSS-SSDBSS), the maximal difference amounts to about 5%. Besides, it is clear from Fig. 7 that in the case of SSSS, the maximum theoretical and experimental hourly outputs amount to 291 and 281 ml/m^2.hr, respectively, and they occur at 14:00. As to the SSDBSS, the upper basin's maximum hourly theoretical and experimental productivity are 328 and 320. The lower basins are 127 and 120 ml/m^2 hr, respectively, coming about at 14:00.

Figs. 8 and 9 show the daily experimental and theoretical accumulated productivity rates of freshwater from 07:00 to 20:00 for the two tested solar still configurations for 2 cm, 3 cm, 4 cm, and 5 cm water depths d_s/equivalent water depths d_e. Figs. 8 and 9 show clearly that the accumulated productivity rate depends on water depth d_s/d_e in both solar still configurations. The accumulated productivity of freshwater increases with decreasing water depth d_s/d_e. This increase is because of the growth in the water temperature inside the basin, which results in greater evaporation and condensation distillate output. The value of accumulated output water of the SSDBSS is higher than that of the SSSS for different water depths d_s/equivalent water depths d_e. Also, the results indicate that the daily experimental and theoretical accumulated productivities of the SSDBSS are 2855 ml/m^2 and 2965 ml/m^2 for an equivalent water depth d_e of 2 cm, respectively. As to the SSSS, these values are 1785 and 1870 ml/m^2 at water depth d_s of 2 cm, respectively.

Table 3 summarizes the theoretical (predicted) and daily experimental accumulated productivities comparison of the two tested still configurations for different water depths d_s/equivalent water depths d_e. It can be noticed from Table 3 that the predicted and experimental accumulated outcomes are almost equal for all tested water depths d_s/equivalent water depths d_e for the two tested solar stills. The deviations between the experimental and predicted productivities were within 6.6%, which shows acceptable agreement between the experimental results and predicted outcomes. Also, it can be noticed from Table 3 that a rise in the equivalent water depth d_e from 2 cm to 3 cm reduces the accumulated productivity by 14.36% for the SSDBSS. In contrast, a decrease of 25.64% and 32.22% are observed as d_e increases from 2 cm to 4 cm and from 2 cm to 5 cm, respectively. On the other hand, for the SSSS, a decrease in accumulated productivity by 15.41%, 27.17%, and 33.33% are recorded as the water depth d_s increases from 2 cm to 3 cm, 2 cm–4 cm, and from 2 cm to 5 cm, respectively.

Table 4 presents the percentage increase in accumulated outcome for the day of the SSDBSS compared with the SSSS at different tested water depths d_s/equivalent water depths d_e. Table 4 suggests that the raise ratio in the experimental and theoretical daily accumulated outcome of the SSDBSS over that of the SSSS is almost the same. This percentage increase is slightly raised with water d_s/equivalent water depth d_e.

The solar still efficiency signifies the capability of the still in desalinating saltwater. It can be practiced as a parameter that should be maximized to find the optimal still design. Fig. 10 displays the experimental thermal efficiency of the day for the two tested solar still configurations for water depths d_s/equivalent water depths d_e of 2 cm, 3 cm, 4 cm, and 5 cm. From Fig. 10, it can be seen that the daily efficiency is diminished as the water depth in the basin d_s/equivalent water depth d_e is increased for the two tested solar stills. The cause behind this is the decrease in the still daily productivity with increasing d_s/d_e (as shown in Figs. 8 and 9). Additionally, it is evident from Fig. 10 that the daily thermal efficiency of the SSDBSS is always greater than that of the SSSS for equal d_s and d_e; e.g., it is 25% for equivalent water depth d_e of 2 cm in case of SSDBSS, whereas it is 15.5% for water depth ds of 2 cm in case of SSSS.

9. Conclusions

The present work is concerned with designing, fabricating, and testing new solar still configuration, namely single slope double basin solar still (SSDBSS) for desalinating saltwater. For judging the quality of this configuration, its performance was compared with that of conventional solar still (SSSS). Therefore a still of the latter type was also fabricated and tested. For a reasonable comparison of the performances of the two tested still configurations, the amount of saltwater to be distilled was taken to be the same for the two

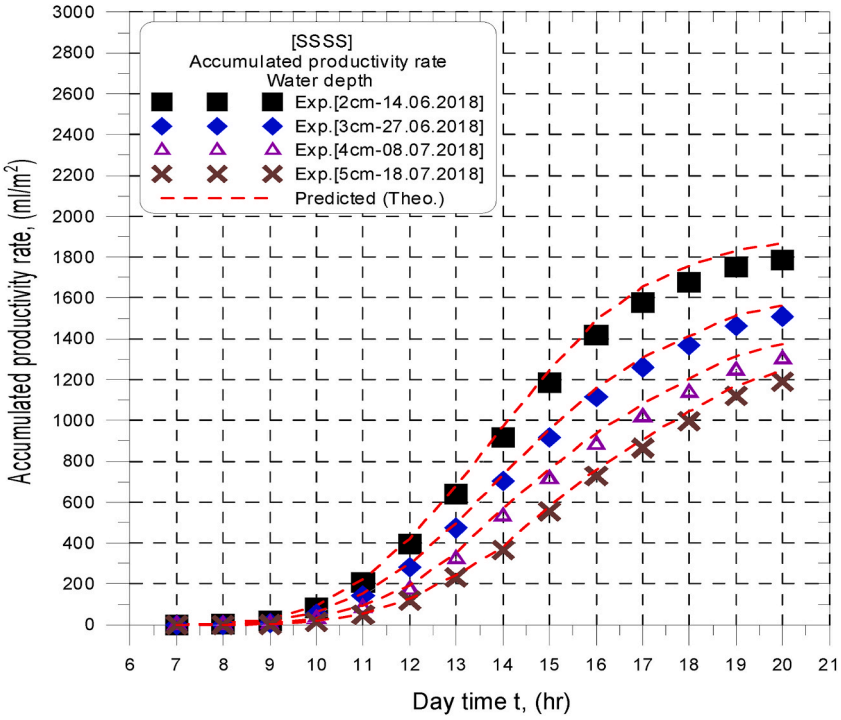

Fig. 8. Experimental and theoretical daily accumulated productivity for SSSS solar still model at different water depths d_s.

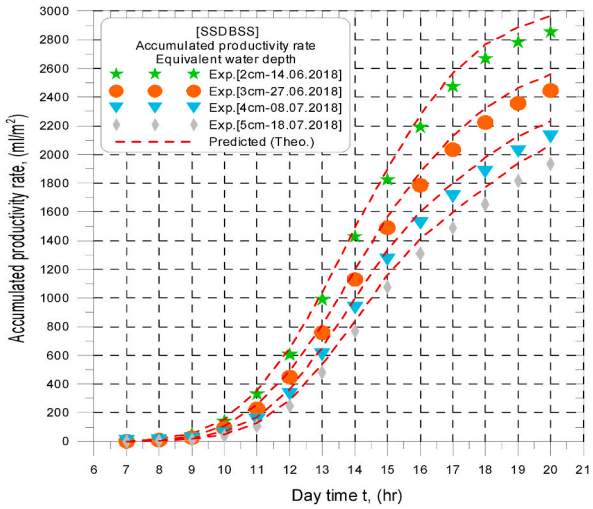

Fig. 9. Experimental and theoretical daily accumulated productivity for the SSDBSS solar still model at different equivalent water depths d_e.

configurations. Thus, a new parameter was introduced in the case of the SSDBSS that is the equivalent water depth. It is half the water depth in the case of the SSSS. Besides the experimental work, a robust analytical model for predicting the performances of both stills was developed. The analysis of the outcomes gained in this work led to draw the following conclusions:

1. The productivity of both solar stills depends mainly on the value of solar irradiation. Its increase causes the water temperature to rise, and the total internal coefficient of heat transfer increases.
2. The SSDBSS configuration has better freshwater productivity than conventional SSSS configuration at all tested water depths. The experimental daily accumulated productivity rate for SSDBSS configuration is 59.9% higher than the conventional SSSS configuration at 2 cm water depth for the test circumstances.
3. The developed model can accurately predict the performance of SSSS and SSDBSS systems within a deviation of ±6.6%.

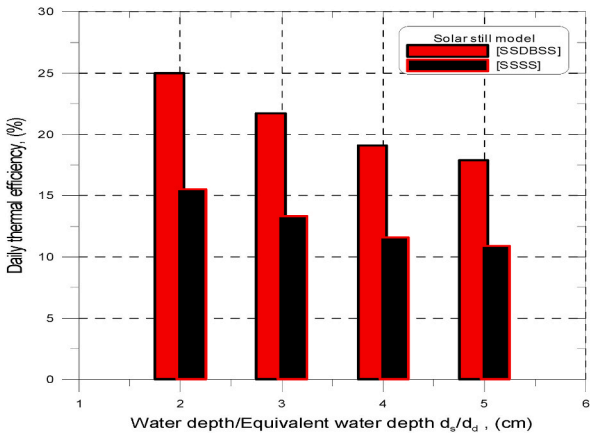

Fig. 10. Daily thermal efficiency for two tested solar still configurations at different water depths/equivalent water depths.

Table 3
Comparison of the theoretical and experimental accumulated productivities for the two tested solar stills at different water depths d_s/equivalent water depths d_e.

Water Depth d_s/Equivalent Water Depth d_e (cm)	Type	Accumulated Productivity (ml/m^2.day)		Deviation (%)
		Exp.	Theo.	
2	SSSS	1785	1870	4.8
	SSDBSS	2855	2965	3.9
3	SSSS	1510	1565	3.6
	SSDBSS	2445	2558	4.6
4	SSSS	1300	1375	5.8
	SSDBSS	2123	2233	5.2
5	SSSS	1190	1245	4.6
	SSDBSS	1935	2063	6.6

Table 4
Percentage increase of the theoretical and experimental daily accumulated productivities for the two tested solar still at different water depths.

Water Depth/Equivalent Water Depth (cm)	Percentage Increase in Accumulated Productivity for SSDBSS Compared to SSSS, (%)	
	Exp.	Theo.
2	59.9	58.6
3	61.9	63.5
4	63.3	62.4
5	62.6	65.7

4. An increase in the water depth d_s/d_e from 2 cm to 3 cm reduces the accumulated productivity by 14.36% for the SSDBSS. In contrast, in the case of SSSS, a decrease of 25.64% and 32.22% are observed as the water depth ds/de increases from 2 cm to 4 cm and from 2 cm to 5 cm, respectively.
5. The experimental thermal daily efficiency of the SSDBSS configuration was 25% at an equivalent water depth of 2 cm, while it is 15.5% for the conventional SSSS configuration at the same water depth (about 61.3% of improvement).

10. Future studies

Based on the experience gained during this work, it is suggested that more work in the following areas can be done:

1. Studying the effect of hot water tank, external and internal reflectors, internal condenser on the performance of SSDBSS.
2. Parametric analysis of the single slope double basin solar still can be done to enhance its productivity and efficiency with the aid of CFD simulation.

Author statement

Conceptualization, methodology and investigation: Mahmoud S. El-Sebaey, Asko Ellman, Ahmed Hegazy, Hitesh Panchal.

Declaration of competing interest

The authors declare that they have no known competing financial interests or personal relationships that could have appeared to

influence the work reported in this paper.

References

[1] F.A. Essa, Z.M. Omara, A.S. Abdullah, S. Shanmugan, Hitesh Panchal, A.E. Kabeel, Ravishankar Sathyamurthy, Wissam H. Alawee, A. Muthu Manokar, Ammar H. Elsheikh, Wall-suspended trays inside stepped distiller with Al2O3/paraffin wax mixture and vapor suction: experimental implementation, J. Energy Storage 32 (2020), 102008.

[2] Hitesh Panchal, Nikunj Patel, Hemin Thakkar, Various techniques for improvement in distillate output from active solar still: a review, 2017, Int. J. Ambient Energy 38 (2) (2017) 209–222.

[3] R. Sathyamurthy, A.E. Kabeel, E.-S. El-Agouz, et al., Experimental investigation on the effect of MgO and TiO_2 nanoparticles in stepped solar still, Int. J. Energy Res. 43 (2019) 3295–3305.

[4] R. Sathyamurthy, A.E. Kabeel, E.-S. El-Agouz, et al., Experimental investigation on the effect of MgO and TiO2 nanoparticles in stepped solar still, Int. J. Energy Res. 43 (2019) 3295–3305.

[5] H. Panchal, A. Awasthi, Theoretical modeling and experimental analysis of solar still integrated with evacuated tubes, Heat Mass Tran. 53 (2017) 1943–1955.

[6] O.O. Badran, H.A. Al-Tahaineh, The effect of coupling a flat-plate collector on the solar still productivity, Desalination 183 (1–3) (2005) 137–142.

[7] Dinesh Mevada, Hitesh Panchal, Kishor Kumar Sadasivuni, Investigation on evacuated tubes coupled solar still with condenser and fins: experimental, exergo-economic and exergo-environment analysis, Case Stud. Therm. Eng. 27 (2021), 101217.

[8] Ammar H. Elsheikh, Hitesh Panchal, Mahmoud Ahmadein, Ahmed O. Mosleh, Kishor Kumar Sadasivuni, Naser A. Alsaleh, Productivity forecasting of solar distiller integrated with evacuated tubes and external condenser using artificial intelligence model and moth-flame optimizer, Case Stud. Therm. Eng. 28 (2021), 101671.

[9] Ali A. Badran, Ihmad A. Al-Hallaq, Imad A. Eyal Salman, Mohammad Z. Odat, A solar still augmented with a flat-plate collector, Desalination 172 (3) (2005) 227–234.

[10] T. Rajaseenivasan, P. Nelson Raja, K. Srithar, An experimental investigation on a solar still with an integrated flat plate collector, Desalination 347 (2014) 131–137.

[11] Samir M. Elshamy, Emad M.S. El-Said, Hitesh Panchal, Hamed R. El-Tahan, Performance assessment of a solar water distiller using circular parabolic absorber: an experimental investigation, Case Stud. Therm. Eng. 28 (2021), 101508.

[12] M.M. Morad, Hend A.M. El-Maghawry, Kamal I. Wasfy, Improving the double slope solar still performance by using flat-plate solar collector and cooling glass cover, Desalination 373 (2015) 1–9.

[13] Ragh Vendra Singh, Shiv Kumar, M.M. Hasan, M. Emran Khan, G.N. Tiwari, Performance of a solar still integrated with evacuated tube collector in natural mode, Desalination 318 (2013) 25–33.

[14] Hitesh Panchal, Petkar Rajan, Chandrakant Sonawane, Kishor Kumar Sadasivuni, Hagar Alm El Din Mohamad, Pradeep Boka, Use of computational fluid dynamics for solar desalination system: a review, Int. J. Ambient Energy (2021), https://doi.org/10.1080/01430750.2021.1965019.

[15] Shiv Kumar, Aseem Dubey, G.N. Tiwari, A solar still augmented with an evacuated tube collector in forced mode, Desalination 347 (2014) 15–24.

[16] Mohammad Behshad Shafii, Mojtaba Shahmohamadi, Meysam Faegh, Hani Sadrhosseini, Examination of a novel solar still equipped with evacuated tube collectors and thermoelectric modules, Desalination 382 (2016) 21–27.

[17] Kamran Mohammadi, Hamed Taghvaei, Ebrahim Goshtasbi Rad, Experimental investigation of a double slope active solar still: effect of a new heat exchanger design performance, Appl. Therm. Eng. 180 (2020), 115875.

[18] Salman H. Hammadi, Integrated solar still with an underground heat exchanger for clean water production, J. King Saud Univ. Eng. Sci. 32 (5) (2020) 339–345.

[19] Poonam Joshi, G.N. Tiwari, Energy matrices, exergo-economic and enviro-economic analysis of an active single slope solar still integrated with a heat exchanger: a comparative study, Desalination 443 (2018) 85–98.

[20] Mahmoud S. El-Sebaey, Hegazy Ahmed, Asko Ellman, Tarek Ghonim, Experimental and CFD study on single slope double basin solar still, Eng. Res. J. Facul. Eng. Menoufia Univ. Part 1 44 (1) (2021) 21–32.

[21] Mahmoud S. El-Sebaey, Asko Ellman, Hegazy Ahmed, Tarek Ghonim, Experimental analysis and CFD modeling for conventional basin-type solar still, Energies 13 (2020) 5374.

[22] Mahmoud S. El-Sebaey, A. Ellman, A. Hegazy, T. Ghonim, An experimental investigation on productivity and performance of an improved design of basin type solar still, in: 21th International Conference on Desalination and Renewable Energy (ICDRE 2019), Copenhagen, Denmark, 11-12 June, 2019.

[23] N. Rahbar, J.A. Esfahani, Estimation of convective heat transfer coefficient in a single-slope solar still: a numerical study, Desalination Water Treat. 50 (2012) 387–396.

[24] O. Badran, M.M. Abu-khader, Evaluating thermal performance of a single slope solar still, Heat Mass Tran. 43 (2007) 985–995.

[25] M.K. Phadatare, S.K. Verma, Influence of water depth on internal heat and mass transfer in a plastic solar still, Desalination 217 (2007) 267–275.

[26] V. Velmurugan, C.K. Deenadayalan, H. Vinod, K. Srithar, Desalination of effluent using fin type solar still, Energy 43 (2008) 1719–1727.